Antarctic Cloud Radiative Forcing at the Surface Estimated from the AVHRR Polar Pathfinder and ISCCP D1 Datasets, 1985–93

MICHAEL J. PAVOLONIS

Cooperative Institute for Meteorological Satellite Studies, University of Wisconsin—Madison, Madison, Wisconsin

JEFFREY R. KEY

Office of Research and Applications, NOAA/NESDIS, Madison, Wisconsin

(Manuscript received 4 June 2002, in final form 11 December 2002)

ABSTRACT

Surface cloud radiative forcing from the newly extended Advanced Very High Resolution Radiometer (AVHRR) Polar Pathfinder (APP-x) dataset and surface cloud radiative forcing calculated using cloud and surface properties from the International Satellite Cloud Climatology Project (ISCCP) D-series product were used in this 9-yr (1985–93) study. On the monthly timescale, clouds were found to have a warming effect on the surface of the Antarctic continent every month of the year in both datasets. Over the ocean poleward of 58.75°S, clouds were found to have a warming effect on the surface from March through October in the ISCCP-derived dataset and from April through September in the APP-x dataset. Net surface fluxes from both datasets were validated against net surface fluxes calculated from measurements of upwelling and downwelling shortwave and longwave radiation at the Neumayer and Amundsen–Scott South Pole Stations in the Antarctic. The net all-wave surface flux from the ISCCP-derived dataset was found to be within 0.4–50 W m^{-2} of the net all-wave flux at the two stations on the monthly timescale. The APP-x net all-wave surface flux was found to be within 0.9–24 W m^{-2}. Model sensitivity studies were conducted to gain insight into how the surface radiation budget in a cloudy atmosphere will change if certain cloud and surface properties were to change in association with regional and/or global climate change. The results indicate that the net cloud forcing will be most sensitive to changes in cloud amount, surface reflectance, cloud optical depth, and cloud-top pressure.

1. Introduction

General circulation model (GCM) simulations have shown that the radiative properties of clouds over the Antarctic greatly influence not only the South Polar climate but global climate as well. For instance, Lubin et al. (1998) found that changes in cloud properties such as effective particle radius and cloud phase lead to dramatic changes in the regional dynamics of Antarctica. In addition, changes in the dynamics of the South Polar region were shown to cause additional dynamic feedbacks that extended well north of the equator. Zonal winds, meridional mass flux, and latent heat release in the Tropics and midlatitudes of the Northern Hemisphere changed significantly when the phase and particle size of clouds over the Antarctic continent were changed to a more realistic regime. Even though differences in the parameterization of Antarctic clouds can lead to much different GCM solutions, relatively little is known about cloud coverage and the bulk physical properties of clouds at high southern latitudes as compared with other regions of the world.

Cloud cover and cloud optical properties will greatly influence the surface radiation budget. For example, Hines et al. (1999) found that the downwelling longwave flux at the surface was up to 50 W m^{-2} too small in National Centers for Environmental Prediction (NCEP) Medium-Range Forecast (MRF) model simulations over the Antarctic because of lower cloud amounts. The mere presence of clouds can greatly alter the downwelling shortwave (SW) and longwave (LW) radiation reaching the surface. Under cloudy conditions, the SW radiation reaching the surface is reduced because of reflection by cloud particles. In converse, clouds absorb LW radiation emitted by the surface and atmosphere and emit radiation toward the surface. Because the emissivity of clouds is greater than the emissivity of the clear atmosphere, the downwelling LW radiation from clouds will be greater than the downwelling radiation from the clear atmosphere. Tsay (1986) predicted that a carbon dioxide doubling in the Arctic would only increase the downwelling LW flux by 4–7 W m^{-2}; Tsay et al. (1989) showed that a low-level stratus cloud increases the downwelling LW by about 80 W m^{-2} when

Corresponding author address: Michael Pavolonis, 1225 West Dayton St., Madison, WI 53706.
E-mail: mpav@ssec.wisc.edu

compared with the clear sky. In addition, Zhang et al. (1996) showed that the presence of persistent cloud cover can cause the onset of snowmelt in the Arctic to occur as much as a month earlier than under clear-sky conditions. Because high-latitude clouds are often less bright than the underlying surface and downwelling SW radiation is small because of large solar zenith angles, the LW effect of clouds at the surface can often dominate the SW effect, causing the surface to warm. Measurements of radiative fluxes by Ambach (1974) at the surface of the Greenland ice sheet showed that the daily net radiation balance (i.e., daily net SW radiation + daily net LW radiation) at the surface in midsummer was about 23 W m^{-2} greater under 100% cloudy conditions when compared with clear-sky conditions.

Surface-based measurements of radiant fluxes, cloud coverage, and cloud radiative properties over the Antarctic continent are limited in time and space and are virtually nonexistent over the ocean areas. Satellite-derived cloud and surface properties from the National Oceanic and Atmospheric Administration (NOAA) polar-orbiting satellites can provide much greater spatial resolution than ground-based stations, although scene identification and cloud masking from satellites in regions covered by snow and ice are problematic (Li and Leighton 1991). Clouds can often be warmer than the underlying surface over Antarctica, and so cloud detection using solely the five spectral channels (0.6, 0.9, 3.7, 11, and 12 μm) available on the Advanced Very High Resolution Radiometer (AVHRR) instrument on the NOAA polar orbiters may be ineffective at times, although techniques such as time series cloud masking, as described in Key (2002), are useful for discerning clouds from the surface in the polar regions. Regardless, satellite-derived datasets are very useful for studying spatial and temporal trends in a given parameter such as cloud radiative effect (commonly referred to as cloud forcing).

It is also important to understand the sensitivities of cloud forcing at the surface to changes in various surface and cloud parameters. Parameters such as surface reflectance, surface temperature, cloud fraction, cloud-top height, cloud optical depth, cloud-particle effective radius, and cloud liquid/ice water content will potentially influence the net radiation balance at the surface (Curry and Ebert 1992). It would be useful to determine which of those parameters would most dramatically alter the net effect of clouds on the surface radiation budget if it were to change. Further, a better understanding of the sensitivities of cloud radiative forcing is needed to gain a better appreciation of the sensitivity of the Antarctic climate to global-scale and local changes in climate.

In this study, the effect of clouds on the surface radiation budget of the Antarctic will be examined theoretically, with a radiative transfer model, and through an examination of two satellite datasets. The spatial and temporal variability of the SW, LW, and net cloud forcing at the surface will be described on a monthly time-scale. Surface fluxes from both satellite-derived datasets will be validated against measurements taken at two Antarctic stations to assess the validity of the satellite-derived cloud forcing.

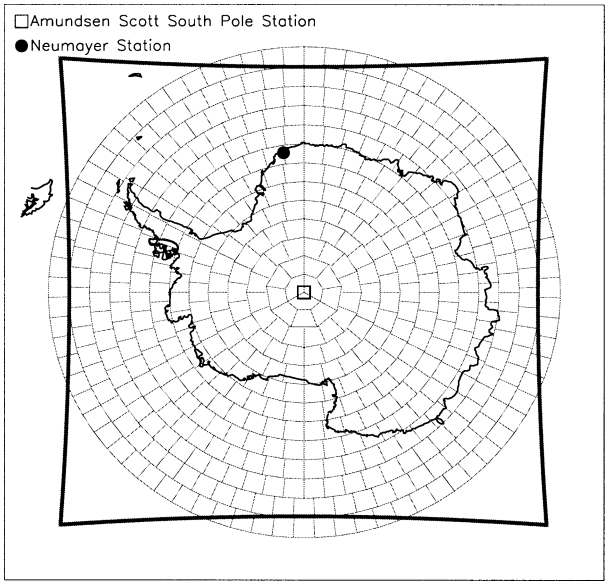

FIG. 1. The ISCCP grid cells south of 57.5°S and the outer boundaries (thick black line) of the APP-x Southern Hemisphere domain. The locations of Amundsen–Scott South Pole Station and Neumayer Station are also shown.

2. Satellite datasets

Data from the AVHRR on the NOAA polar-orbiting satellites were used to derive the AVHRR Polar Pathfinder (APP) dataset (Meier et al. 1997; Maslanik et al. 1998, 1999). The standard APP products include spectral radiance, viewing and illumination geometry, three cloud masks, and clear-sky surface temperature and albedo sampled at a 5-km resolution into two daily composite images covering both polar regions. The APP product has been expanded recently to include cloud properties, radiative fluxes, and cloud forcing on a 25-km scale for two daily composite images (the APP-x product). The composite times are 0200 and 1400 local solar time (LST), with most of the observations falling within 1 h of those times. The boundaries of the APP-x domain are shown in Fig. 1. Surface temperature is calculated with a split-window infrared algorithm. Surface albedo retrieval for clear and cloudy skies employs corrections for anisotropic reflectance and atmospheric effects (Key et al. 2001). Cloud detection is done with a variety of spectral and temporal tests optimized for high-latitude conditions. Cloud particle phase uses near-infrared reflectances (daytime) and infrared brightness temperature differences to separate ice and liquid (''water'') clouds (Key and Intrieri 2000). Cloud optical depth and particle effective radius retrievals use absorbing and nonabsorbing wavelengths, where the absorbing wave-

length is more sensitive to particle size and the nonabsorbing wavelength is more sensitive to optical depth. Cloud temperature is calculated from the infrared window brightness temperature, adjusted for surface emission if the cloud transmittance is greater than 1%. The retrieved cloud and surface parameters are then used as input to FluxNet, a neural-network implementation of the Streamer two-stream radiative transfer model (Key and Schweiger 1998) for the calculation of radiative fluxes. Shortwave and LW fluxes and cloud forcing at the surface and the top of the atmosphere were computed with FluxNet because of its computational efficiency: it is up to 10 000 times as fast as Streamer. A comparison between Streamer and FluxNet using 5000 test cases showed that the root-mean-square errors associated with FluxNet are less than 3% of the mean downwelling and upwelling SW and LW flux values (Key and Schweiger 1998). For algorithm details, see Key (2002).

A second satellite dataset is the International Satellite Cloud Climatology Project (ISCCP) cloud product (Schiffer and Rossow 1983). Five geostationary and two polar-orbiting satellites are used to collect data that are then processed into global cloud datasets. The latest series of ISCCP datasets is the D series. Algorithms used to create the earlier C-series datasets have been shown to underestimate cloud amount, especially in the polar regions (Rossow et al. 1996). However, the ISCCP D-series retrieval algorithms incorporate improved methods for cloud detection over the polar regions. For instance, the algorithms have been adjusted so as better to detect cold clouds and clouds over snow and ice through the added use of AVHRR channel 3 (3.7 μm). Schweiger and Key (1994) speculated that the ISCCP C series missed thin, low clouds in the polar regions. In the D-series dataset, cloud amounts are greater and cloud optical depths are smaller when compared with the C series and both are believed to be more realistic (Key et al. 1999).

In this study, cloud and surface properties from the ISCCP D-series dataset were used as input to a radiative transfer model that computed SW and LW radiant fluxes at the surface and the top of the atmosphere (TOA) and surface and TOA cloud radiative forcing for 1985–93. Only surface fluxes and surface cloud radiative forcing will be discussed in this study. As with the calculation of radiative fluxes with the APP-x data, cloud, atmospheric, and surface parameters from the ISCCP 3-hourly dataset (D1) were used as input to FluxNet. For more information concerning the ISCCP D1 dataset, see Rossow et al. (1996). Temperature and humidity profiles from the Television and Infrared Observation Satellite (TIROS) Operational Vertical Sounder (TOVS) Pathfinder Path-P dataset (Francis and Schweiger 2000) were used when and where available, primarily around the Antarctic continent, because Path-P retrievals are not done over high-elevation surfaces. The fluxes and cloud forcing were computed every 3 h for both the Arctic and Antarctic poleward of 58.75°N and 58.75°S, respectively. Refer to Pavolonis (2002) for more specific details concerning the ISCCP-derived dataset. Figure 1 shows the ISCCP grid cells for the Antarctic.

Using a 9-yr average over the period of 1985–93 for both the ISCCP and APP-x datasets, the spatial and temporal variability of surface cloud forcing and surface and cloud properties were analyzed. Cloud forcing is defined as the integrated partial derivative of the SW or LW radiative flux, such that

$$\mathrm{CS} = \int_0^{A_c} \frac{\partial S_s}{\partial a}\, da = S_s(A_c) - S_s(0),$$

$$\mathrm{CL} = \int_0^{A_c} \frac{\partial L_s}{\partial a}\, da = L_s(A_c) - L_s(0), \quad \text{and}$$

$$\mathrm{CNET} = \mathrm{CS} + \mathrm{CL}, \tag{1}$$

where CS, CL, and CNET are the SW, LW, and net cloud forcing at the surface, respectively, A_c is the total cloud amount, S_S and L_S are the net SW and LW fluxes at the surface, and a is cloud fraction. The net SW flux is defined as the difference between the downwelling SW flux and the upwelling SW flux. The net LW flux is similarly defined as the difference between the downwelling LW flux and the upwelling LW flux. In both cases, the downwelling and upwelling fluxes are taken to be positive. The net cloud forcing is simply the sum of the SW and LW cloud forcing. When the cloud forcing is positive, clouds have a warming effect; clouds will have a cooling effect when the cloud forcing is negative.

3. Results

To evaluate both spatial and temporal trends in cloud amount and cloud forcing from the APP-x dataset, zonal averages were calculated for each 2.5° latitude interval from 90° to 57.5°S. Only monthly means corresponding to the APP-x composite time of 1400 LST will be discussed. This is because 1400 LST is much closer to local solar noon than is 0200 LST; thus, the magnitude of the SW component of the surface cloud forcing will be much larger than at 0200 LST, and it would be useful to determine the radiative impact of clouds on the surface when the SW contribution to the CNET is relatively large during the summer months. In addition, to evaluate both spatial and temporal trends in the monthly mean (based on daily averages) cloud amount from the ISCCP D2 dataset and cloud forcing from the ISCCP-derived dataset, zonal averages were calculated for each 2.5° latitude interval from 88.75° to 58.75°S in the ISCCP dataset for each month. Each of these latitudes represents the center of the ISCCP grid cells under consideration.

The top of Fig. 2 shows the spatial and temporal variability of the zonally averaged monthly cloud amount in the Antarctic as given by the APP-x dataset. The largest monthly cloud amounts are generally found

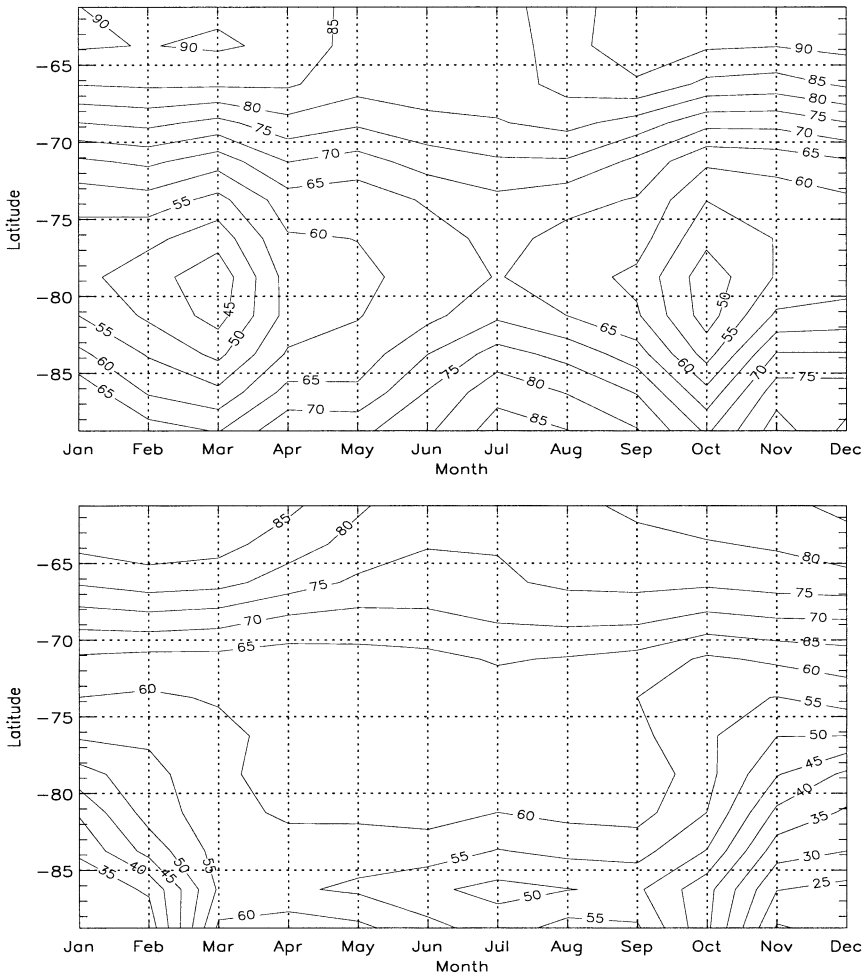

FIG. 2. The spatial and temporal distribution of mean monthly cloud amount (%) from the (top) APP-x dataset at 1400 LST and (bottom) ISCCP D2 dataset (1985–93) for the Antarctic.

over the ocean areas north of 70°S. Further, the seasonal variation in cloud amount is less than 10% northward of about 72°S. In converse, at higher latitudes, the monthly cloud amount may vary by as much as approximately 20% throughout the year.

The bottom of Fig. 2 shows the spatial and temporal variability of the zonally averaged monthly cloud amount from the ISCCP D2 dataset. Monthly cloud amounts are lowest poleward of about 85°S during the austral summer; the ISCCP cloud amounts typically increase with distance from the South Pole. The largest monthly cloud amounts are always found over the ocean areas north of 70°S. Further, the month-to-month variation in cloud amount is less than 10% north of 75°S. At higher latitudes, the monthly cloud amount may vary by as much as 25%–30%. This result is similar to the result given by the APP-x dataset. However, a large difference exists poleward of about 80°S during the summer months when the monthly average cloud amount from the APP-x dataset is 20%–50% greater than the ISCCP D2 cloud amounts.

The top of Fig. 3 shows that the CS in the APP-x dataset greatly decreases (becomes more negative) very sharply during the summer months from 80°S northward because of the decrease in surface albedo and solar zenith angle away from the Pole. The CS poleward of 80°S is always greater than -15 W m^{-2}. At lower latitudes, the presence of clouds can lead to more than 200 W m^{-2} of cooling in the SW at the surface. During the Antarctic winter, clouds cause less than 5 W m^{-2} of cooling over much of the latitude range because of very large solar zenith angles and an increase in surface albedo over the ocean caused by more widespread sea ice.

In a similar way, the CS from the ISCCP-derived dataset also decreases away from the Pole (Fig. 3, bottom). The largest gradient in CS occurs away from the Pole during the Antarctic summer months as a result of the transition from a sea-ice surface to an open-water surface. The CS poleward of 80°S never becomes more negative than 20 W m^{-2}. The magnitude of the CS from the ISCCP-derived dataset is generally smaller than the

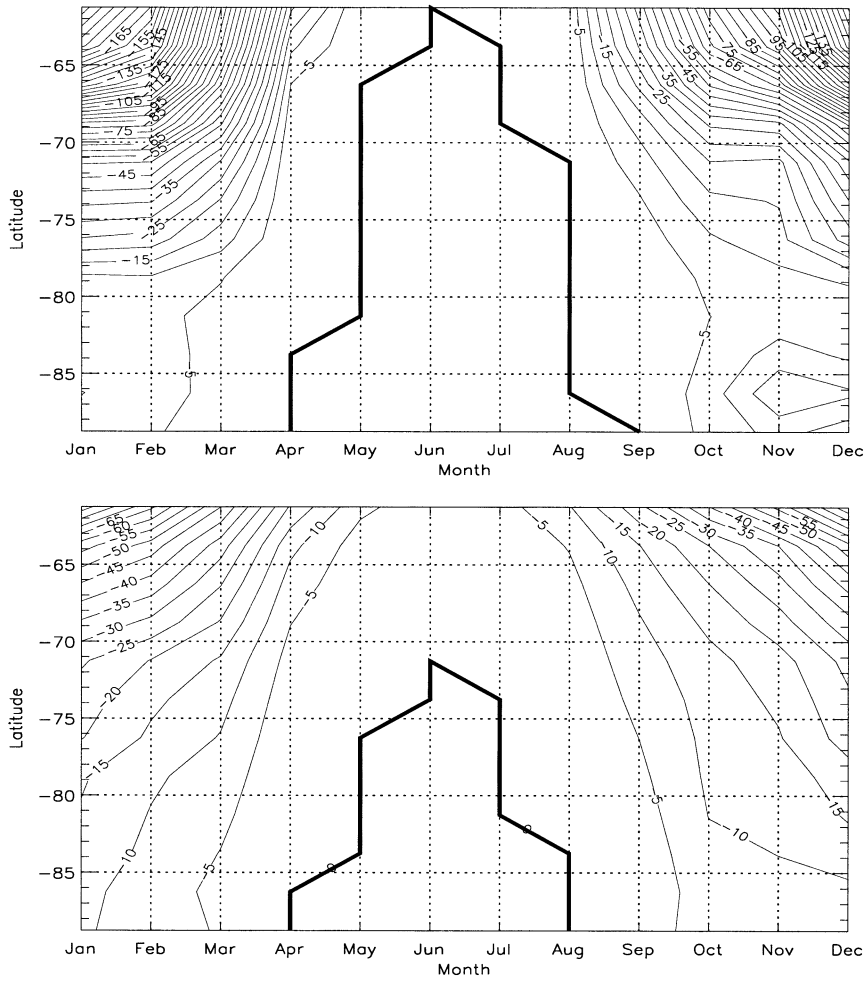

FIG. 3. The spatial and temporal distribution of the mean monthly SW cloud forcing at the surface (W m^{-2}) from the (top) APP-x dataset at 1400 LST and (bottom) ISCCP-derived dataset (1985–93) for the Antarctic. The thick black contour represents 0 W m^{-2}.

CS from the APP-x data, especially away from the Pole, because sunlight is present around the APP-x observation time of 1400 LST that is stronger than that averaged over the course of the day. Further, poleward of about 83°S during the months of November and December, the larger cloud amounts given by the APP-x dataset (as compared with the ISCCP dataset) likely cause the SW cooling effect of clouds to be greater in the APP-x dataset.

North of 75°S, the CL from the APP-x dataset does not vary much from season to season (Fig. 4, top) largely because the monthly cloud amount does not exhibit a strong seasonal cycle at these latitudes. At higher latitudes, the surface CL has more seasonal variability. Poleward of 75°S, the APP-x CL is greatest in summer and is at a minimum in autumn and spring; the ISCCP-derived CL is greatest in winter and is at a minimum in the summer (Fig. 4, bottom). The largest values of the CL are found in the spring north of 65°S, where cloud amounts are high. The seasonal variability of the CL at higher latitudes in the APP-x dataset is largely due to seasonal changes in mean cloud amount, because patterns in cloud amount closely match the patterns in the CL. The differences in the CL between the two datasets can be partly explained by differences in cloud amount. In addition, the APP-x cloud-top pressures are larger than the ISCCP D2 cloud-top pressures over the entire range of latitude and time by about 30–150 hPa (not shown). Because the vertical location of the clouds in the APP-x dataset is on average lower (warmer) than that of the clouds in the ISCCP D2 dataset, the APP-x CL will be greater if the distribution of cloud optical depth from both datasets is similar. Over much of the latitude range of interest, the cloud optical depth from both datasets is similar during the summer (not shown). When no sunlight is present, cloud optical depth is not retrieved during the ISCCP processing and so interpolated values are used.

In the APP-x data, at latitudes poleward of about 76°S, clouds were found to have a warming effect on

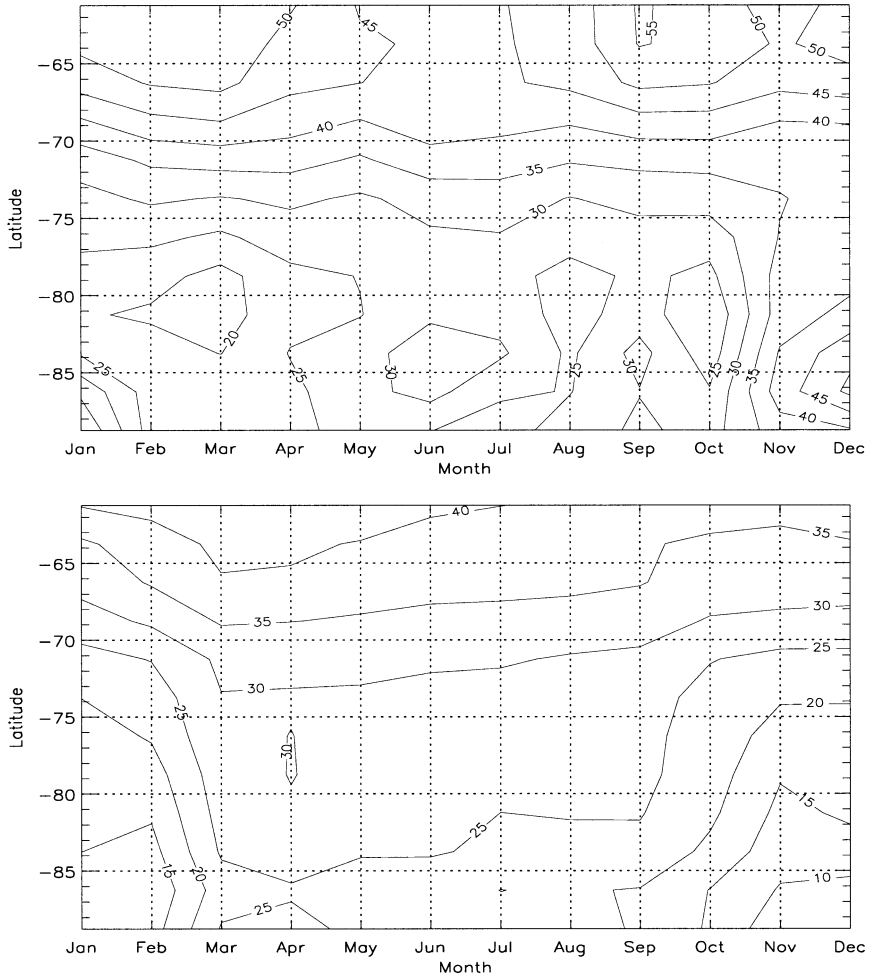

FIG. 4. The spatial and temporal distribution of the mean monthly LW cloud forcing at the surface (W m^{-2}) from the (top) APP-x dataset at 1400 LST and (bottom) ISCCP-derived dataset (1985–93) for the Antarctic.

the surface for every month of the year (Fig. 5, top). Because of the high-albedo surface over the Antarctic continent, which is prominent throughout the year, and large solar zenith angles, the magnitude of the CS is small enough so that the magnitude of the CL is equal to or greater than the magnitude of the CS. The maximum in the CNET occurs during the winter at all latitudes. In addition, the CNET typically increases away from the South Pole during the winter and decreases away from the Pole during the summer. A maximum warming of 40 W m^{-2} is seen during the winter north of 70°S. The minimum CNET when averaged over all of the pixels over the Antarctic continent is 16 W m^{-2}, which occurs in March, and the maximum is 30 W m^{-2} in July. Over the ocean, the minimum is −134 W m^{-2} in January and 46 W m^{-2} in June and July.

The ISCCP-derived data indicate that, at latitudes poleward of about 80°S, clouds were found to have a warming effect on the surface for almost every month of the year (Fig. 5, bottom). The exception occurs in November and December near the Pole because of very small cloud amounts. Note that, even though the CL generally decreases poleward, the CL is still greater than the CS. The minimum CNET when averaged for all grid cells over the Antarctic continent is 0.04 W m^{-2} in December and the maximum is 26 W m^{-2} in April and May. In a similar way, over the ocean, the minimum is −30 W m^{-2} in January and the maximum is 38 W m^{-2} in June. It is interesting to note that this warming effect is typically smaller than that seen in the APP-x CNET data largely because the CL from the APP-x dataset is usually larger. At latitudes north of about 75°S, comparisons between the APP-x and ISCCP-derived data are unfair because the incoming solar radiation at 1400 LST is much greater than the daily average of incoming solar radiation. At higher latitudes, this difference will be less during the summer because these locations are illuminated at nearly all times.

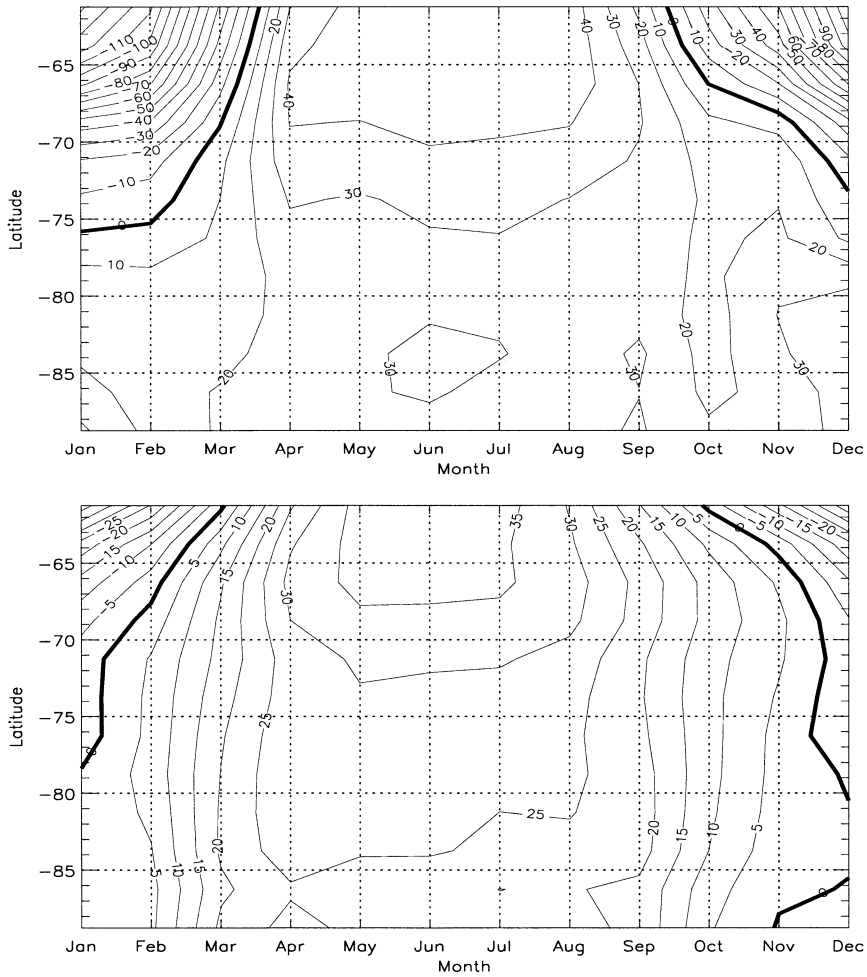

FIG. 5. The spatial and temporal distribution of the mean monthly net cloud forcing at the surface (W m^{-2}) from the (top) APP-x dataset at 1400 LST and (bottom) ISCCP-derived dataset (1985–93) for the Antarctic. The thick black contour represents 0 W m^{-2}.

4. Validation

Two stations were chosen for comparisons with measured surface fluxes as a way of assessing the accuracy of the ISCCP-derived and APP-x-derived surface cloud forcing. Direct surface-based measurements of cloud forcing are not available, and so the relative accuracy of the ISCCP-derived and APP-x cloud forcing products were determined by comparing the all-sky net SW, net LW, and net all-wave surface fluxes from the ISCCP-derived and APP-x datasets with all-sky net surface fluxes calculated from surface measurements of upwelling and downwelling SW and LW radiation at the Neumayer Station and the Amundsen–Scott South Pole Station in Antarctica.

Neumayer Station is located on the Ekström Ice Shelf in the northeast Weddell Sea at 71°S, 8°W. The location of Neumayer Station is also shown in Fig. 1. Surface flux measurements at Neumayer Station were obtained from the Alfred Wegener Institute for Polar and Marine Research for 1993. This year was chosen for the comparison because there were not many missing measurements in the Neumayer data as compared with years previous to 1993. The error in the total radiation budget based on the measurements is thought to be less than 5 W m^{-2} (G. König-Langlo 2002, personal communication). Monthly means of the upwelling and downwelling SW, LW, and net surface fluxes were averaged from two nearby ISCCP grid cells and were compared with the monthly means from Neumayer Station. When comparing the APP-x surface fluxes with the fluxes measured at Neumayer, an average of two nearby APP-x pixels was calculated (each APP-x pixel is 25 km) for the monthly mean of each composite time of 0200 and 1400 LST, and then a ''daily'' mean was calculated by averaging the data from the two local solar composite times. Monthly means of hourly data that correspond to 0200 and 1400 LST at Neumayer Station (based on the longitude of Neumayer Station) were calculated for each composite time, and a daily average from the monthly means of the two APP-x composite times was calculated for comparison with the APP-x surface fluxes.

The second station chosen is the Amundsen–Scott South Pole Station. The South Pole Station measurements were taken by Dutton et al. (1989) from April of 1986 to February of 1988. The approximate absolute errors in the measurements reported by Dutton et al. (1989) are 2% for the SW measurements and 5% for the LW measurements. The three ISCCP grid cells, each of which is centered on 88.75°S, that surround the South Pole were chosen for this comparison. The South Pole is surrounded by a region of relatively uniform snow and ice in almost all directions for about 200–300 km. The centers of all three of the ISCCP cells used are within 139 km of the South Pole, and so the monthly mean of measurements made at Amundsen–Scott South Pole Station should be well-suited for comparison with the spatial average of monthly means from the three ISCCP grid cells. To compare the APP-x surface fluxes with the fluxes measured at South Pole Station, daily averages based on the monthly means for the two APP-x composite times were computed for three APP-x pixels that surround the South Pole within 19 km. The average of these three APP-x pixels was compared with a daily average, based on 24 hourly measurements, at the South Pole Station. The three APP-x pixels are centered at three different longitudes, which are characterized by three different universal coordinated times (UTC) for each APP-x local solar composite time. In addition, the change from one UTC time zone to another occurs over a relatively small distance for a given latitude near the Pole, and thus the use of a daily average of the South Pole data in these comparisons is justifiable.

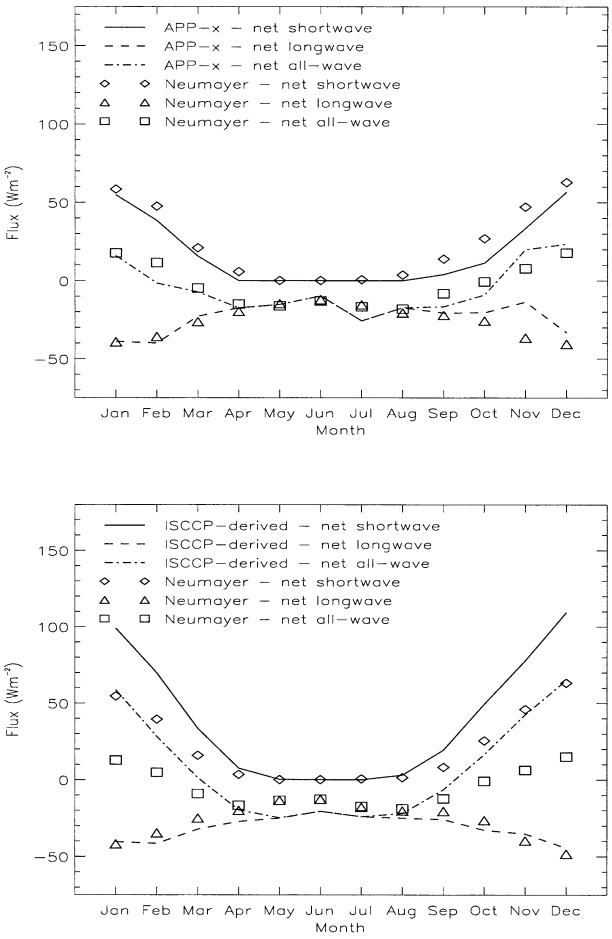

FIG. 6. Comparison of the surface net SW, LW, and all-wave radiative fluxes from the (top) APP-x dataset and (bottom) ISCCP-derived dataset and the net fluxes based on surface measurements made at Neumayer Station (1993).

a. Neumayer Station

The error/bias discussed in this section and in the sections to follow is defined as the difference between the satellite-derived flux and the measured flux. The top of Fig. 6 shows the comparisons between the APP-x net surface fluxes and net surface fluxes computed from the upwelling and downwelling SW and LW fluxes measured at Neumayer Station. The magnitude of the error in the net SW flux is less than 10 W m^{-2} for every month except October (-16 W m^{-2}) and November (-14 W m^{-2}). The largest error in the net LW flux is $+23$ W m^{-2} in November. The error in the net LW flux is less than 11 W m^{-2} in all other months. The net surface radiation balance is within 9 W m^{-2} of the Neumayer net all-wave flux for every month except February (-13 W m^{-2}) and November ($+12$ W m^{-2}). In general, discrepancies exist with the downwelling and upwelling components of the SW and LW surface fluxes (not shown); however, these errors tend to cancel each other out so that the net all-wave surface flux is within 13 W m^{-2} for every month of the year. For instance, in January, the downwelling and upwelling SW flux are underestimated by 89 and 85 W m^{-2}, respectively. These large underestimates are due mainly to differences between the solar zenith angle at the location at which the measurements were taken and the solar zenith angle used in the APP-x calculations. This difference in solar zenith angle arises from the fact that the actual APP-x observation time may differ by as much as 2 h from either of the APP-x reference times of 0200 and 1400 LST. Because comparisons between the APP-x cloud amount and surface observations of cloud amount at Neumayer Station agree to within about 8% during the summer (Pavolonis 2002), most of the error in the downwelling SW flux (and, hence, the upwelling SW flux) will be a result of differences in solar zenith angle. Calculations show that even a difference of 0.5 h can change the solar zenith angle by about 3° in the summer at the latitude of Neumayer Station. Minnett (1999) showed that the incident SW flux measured at the surface in the Arctic often decreased by more that 50 W m^{-2} when the solar zenith angle decreased by about 3°, for a variety of atmospheric conditions. This comparison suggests that the solar zenith angle at the time of the satellite overpass is at least somewhat larger than the solar zenith angle at the time of the measurements at

Neumayer Station. In the LW range, the downwelling and upwelling fluxes are underestimated by 5 and 7 W m^{-2}, respectively, in January.

The bottom of Fig. 6 shows the comparisons between the ISCCP-derived net surface fluxes and net surface fluxes computed from the upwelling and downwelling SW and LW fluxes measured at Neumayer Station. The net SW flux at the surface as given by the ISCCP-derived dataset has a positive bias during the austral summer months that is as large as about 44 W m^{-2}. This bias is due primarily to the large negative bias (77 W m^{-2} in January) that exists in the upwelling SW flux, although the smaller negative bias (33 W m^{-2} in January) in the downwelling SW flux partially offsets the upwelling SW flux bias. In other words, the large positive bias in the summer occurs because the upwelling SW flux is significantly underestimated relative to the downwelling SW flux, which is not the case with the APP-x data. However, similar to the APP-x data behavior, the downwelling SW flux from the ISCCP-derived dataset shows a significant negative bias largely because of solar zenith angle differences. In the LW, the negative biases seen in both the downwelling and upwelling LW fluxes are similar, and so the bias in the net LW flux is less than 8 W m^{-2}, with the exception of May, for which a negative bias of 12 W m^{-2} is observed. The net LW flux has a negative bias from February through October and a positive bias during all other months. Note, however, that both the downwelling LW flux and upwelling LW flux are characterized by a large negative bias every month of the year. Both the APP-x and ISCCP D2 cloud amounts have been shown to be within 17% of surface observations made at Neumayer Station for nearly every month of the year (Pavolonis 2002). Thus, a large cold bias in the retrieved cloud temperature may explain much of the negative bias in the downwelling LW flux derived from the ISCCP-derived dataset. However, because Neumayer Station is in a region of highly varying topography, comparisons of large grid cells to point measurements are difficult and may lead to errors. The net all-wave flux is characterized by a large bias of up to +50 W m^{-2} during the austral summer months because of large errors in the net SW flux during this same time period. From March through September, the errors in the net all-wave flux are less than 12 W m^{-2}.

b. South Pole Station

Figure 7 shows the comparisons between the APP-x net surface fluxes and net surface fluxes computed from the upwelling and downwelling SW and LW fluxes measured at the South Pole Station. During the summer months, errors in the net SW flux are large, mainly because of errors in the downwelling SW flux (not shown). A negative bias in the net SW flux in excess of 20 W m^{-2} is seen in December (1986), November (1987), and January (1987). During those months, the downwelling SW flux is underestimated and the downwelling LW flux is overestimated. These errors correspond to a positive bias in retrieved cloud amount as compared with surface observations made at South Pole Station (Pavolonis 2002). The signs of the errors in the downwelling and upwelling LW flux do not always agree (not shown), and so errors in the net LW flux can be as high as about 37 W m^{-2}. When the SW and LW components of the surface radiation balance are combined, errors in the SW and LW components have a tendency to at least partially cancel each other out. Thus, the errors in the net all-wave surface flux are less than 17 W m^{-2} for every month except April of 1987 (−23.9 W m^{-2}).

Figure 7 also shows the comparison between the ISCCP-derived net surface fluxes and the net surface fluxes computed from the upwelling and downwelling SW and LW fluxes measured at South Pole Station. The ISCCP-derived net SW flux is 12–41 W m^{-2} greater than the net SW flux calculated from the downwelling and upwelling SW fluxes taken from measurements made at the South Pole Station from November through February. This difference is due mainly to a large negative bias in the upwelling SW flux (not shown), which suggests that the surface albedo that is used when calculating the SW fluxes is too small. In the LW range, the ISCCP-derived net flux is within 18 W m^{-2} of the net LW flux derived from measurements of the downwelling and upwelling LW fluxes. Because errors in the upwelling and downwelling LW flux tend to be of the same sign, the maximum error in the net LW flux is not as large as the maximum error in either the downwelling or upwelling LW flux (not shown). Note that, during the summer, both the downwelling LW flux and the cloud amount generally exhibit a negative bias (Pavolonis 2002). Recall that cloud amount tends to be overestimated at the South Pole in the summer in the APP-x dataset. The cloud amounts from the two datasets are different because the cloud-mask techniques differ. The single-image cloud detection tests and thresholds used in the APP-x processing are specifically derived for the polar regions and may differ from the tests and thresholds used in the ISCCP processing. The ISCCP algorithm also includes a spatial variability test whereas the APP-x does not. The ISCCP-derived net all-wave flux has errors as large as 50 W m^{-2}, primarily because the errors in the net SW flux are large during the summer.

5. Sensitivity studies

It is important to understand how the surface radiation budget in a cloudy atmosphere will change if certain cloud and surface properties were to change in association with local and/or global climate change. It would also be useful to determine some general threshold values of solar zenith angle and surface albedo for which the sign of the net cloud forcing at the surface will change. Using the Streamer radiative transfer model

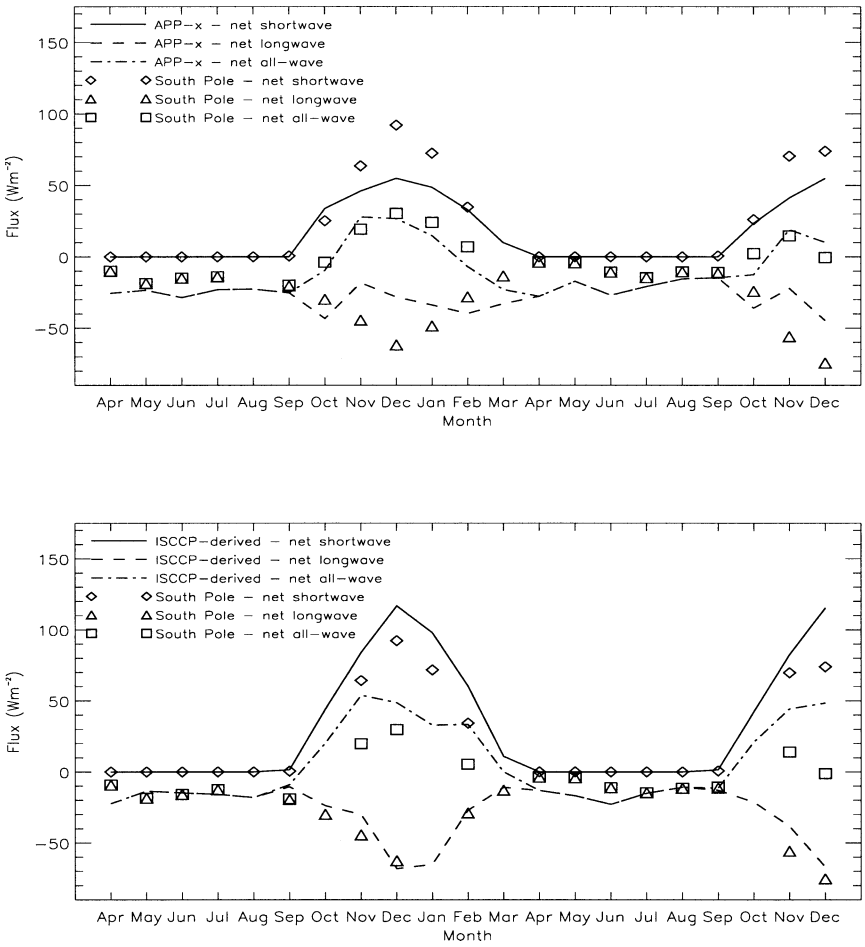

FIG. 7. Comparison of the surface net SW, LW, and all-wave radiative fluxes from the (top) APP-x dataset and (bottom) ISCCP-derived dataset and the net fluxes based on surface measurements made at South Pole Station (Apr 1986–Dec 1987).

(Key and Schweiger 1998), model sensitivity studies were conducted to determine the relative importance of various cloud and surface properties in determining the value of the SW, LW, and net cloud radiative forcing at the surface. More specific, the sensitivity of the SW, LW, and net cloud forcing to changes in cloud fraction, cloud-top pressure, cloud optical depth, particle effective radius, liquid/ice water path, solar zenith angle, surface albedo, and surface temperature was examined.

TABLE 1. Input parameters for cloud-forcing sensitivity studies. For liquid water clouds, an effective particle radius of 10 μm and a liquid water content of 0.2 g m^{-3} are used. For ice clouds, an effective particle radius of 30 μm and an ice water content of 0.07 g m^{-3} are used.

Parameter	Value
Surface emissivity	0.99
Visible surface reflectance	0.61
Solar zenith angle (°)	70.83
Cloud fraction	0.78
Cloud-top temperature (K)	254.1
Cloud-top pressure (hPa)	672.82
Cloud optical depth	7.7
Surface temperature (K)	266.3
Column ozone amount (Dobson units)	350

Shortwave and LW computations were both done using the hemispheric-mean method of Toon et al. (1989). Each of the scenes was modeled using only a single cloud layer. The variation of cloud forcing with respect to a given cloud or surface parameter was calculated for a scene consisting of 73% sea ice and 27% open water with a visible albedo of 0.61, which is typical for a coastal Antarctic location. These values were obtained from the ISCCP D2 dataset. ISCCP D2 average parameters were chosen because the ISCCP monthly averages are based on eight observations per day over the entire spatial domain whereas the APP-x monthly averages are based on two composite observations per day. Table 1 shows the baseline model input parameters obtained from the ISCCP D2 dataset.

Sensitivities were determined for both an all-liquid-phase cloud and an all-ice-phase cloud. Model studies were performed for an ice cloud with a baseline effective

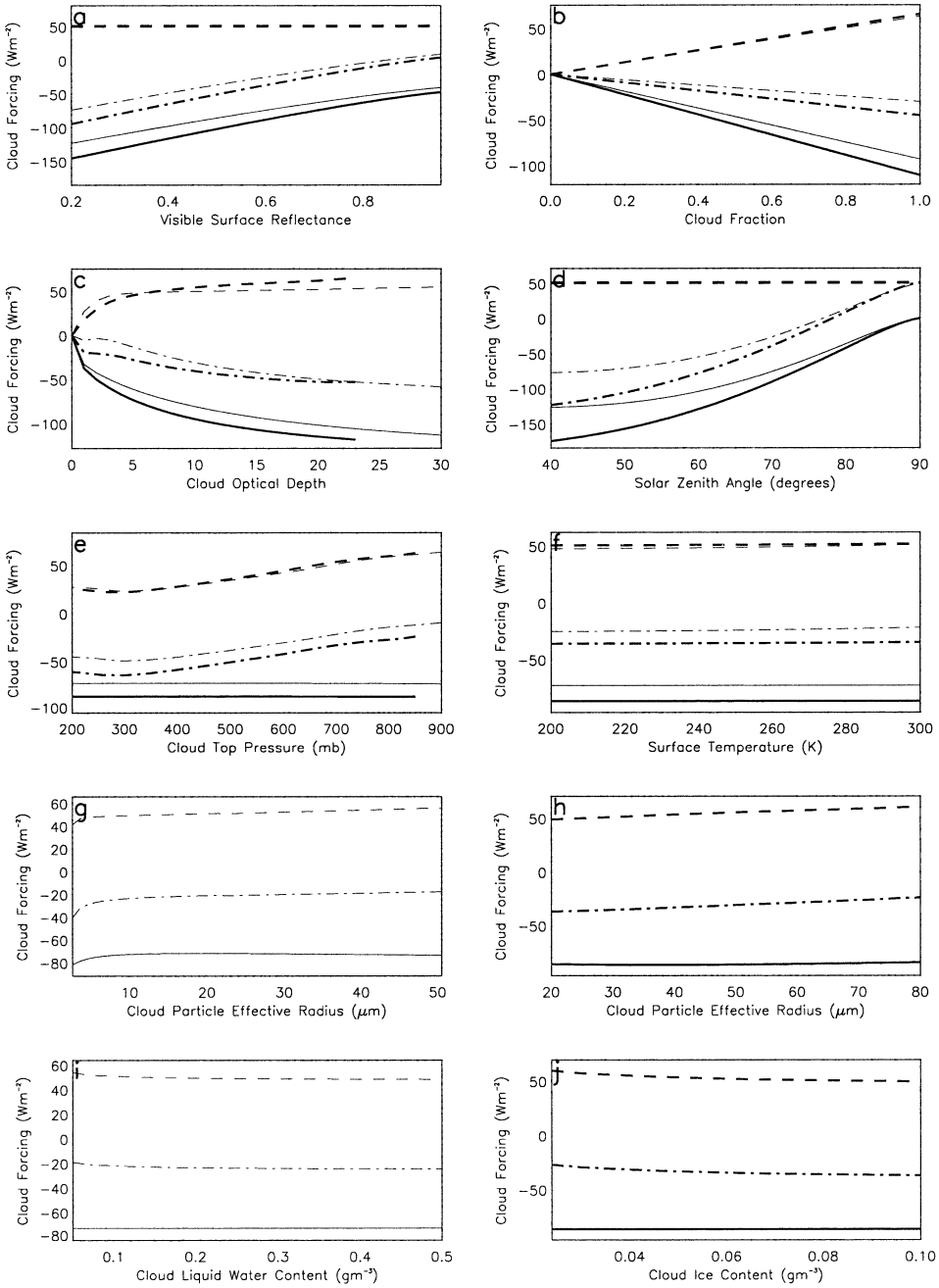

FIG. 8. Shortwave (solid), LW (dashed), and net (dash–dot) surface cloud forcing as a function of several parameters. Calculations were performed for both a single-layered liquid water cloud (thin lines) and an ice cloud (thick lines). Note that calculations were not performed when the cloud base was determined to be below the ground. This condition mainly occurs for ice clouds.

particle radius of 30 μm and a baseline ice water content of 0.07 g m^{-3}. Studies for a liquid cloud with a baseline effective particle radius of 10 μm and a baseline liquid water content of 0.2 g m^{-3} were also performed. These values are the same effective particle sizes and water concentrations used in the ISCCP processing. The temperature and moisture profiles used in this study were taken from radiosonde measurements near the Antarctic coast. A spectrally constant surface emissivity of 0.99 and a column ozone amount of 350 Dobson units were used. The solar zenith angle of 70.83° was determined by averaging the cosine of the daily mean solar zenith angle for the month of January for 2° latitude intervals from 60° to 76°S. The cosines of the monthly mean

solar zenith angles for each latitude range were then averaged to obtain the cosine of the solar zenith angle used in the model calculations.

Only summertime sensitivity studies were conducted so that the LW and SW components of the cloud forcing both could be examined. Furthermore, the relative sensitivity of the CL to various cloud and surface parameters will not change significantly when baseline parameters typical of winter are used as opposed to parameters typical of summer. In other words, the actual magnitudes of the sensitivities will likely be different, but the relationship should not vary much from season to season. The SW, LW, and net cloud forcing were computed for a range of values of each cloud and surface parameter. All other parameters are set to the baseline values. The only exception occurs when the sensitivity of the cloud forcing with respect to cloud-top pressure was investigated. When the cloud-top pressure was changed to a different level in the input profile, the cloud-top temperature was taken to be the temperature at that same level. Figures 8a–j show the trends of the SW, LW, and net cloud forcing at the surface over a range of values of the aforementioned sensitivity parameters.

The CS is not sensitive to surface temperature (Fig. 8f), cloud-top pressure (Fig. 8e), and cloud water content (Figs. 8i,j). Changes in cloud particle size (Figs. 8g,h) only result in fairly small changes in the CS, especially for ice clouds. The CS is only significantly sensitive to changes in cloud particle radius for liquid water cloud particles smaller than 10 μm. The CS is highly sensitive to the parameterization of cloud optical depth (Fig. 8c) for liquid water and ice clouds both, although the magnitude of the CS is generally greater for ice clouds. As is shown in Fig. 8d, the CS has a very large solar zenith angle dependence, especially for ice clouds. The CS is also very sensitive to changes in cloud fraction (Fig. 8b) and visible surface reflectance (Fig. 8a). The magnitude of the CS is greater for ice clouds, especially for larger cloud amounts. Even small changes in visible surface albedo will result in significant changes in the CS.

The CL is not sensitive to changes in visible surface albedo (Fig. 8a) and solar zenith angle (Fig. 8d). The CL is not sensitive to changes in surface temperature (Fig. 8f) because changes in the upwelling LW flux due to a change in surface temperature will occur in the clear-sky and all-sky simulations both, and, thus, changes in the upwelling LW flux will be largely offset. Further, sensitivities to cloud particle radius (Figs. 8g,h) and cloud water content (Figs. 8i,j) are small when compared with the sensitivities with respect to cloud-top pressure (Fig. 8e), cloud optical depth (Fig. 8c), and cloud fraction (Fig. 8b). Increases in the effective particle radius lead to an increase in the CL for liquid water and ice clouds, and decreases in the cloud water content coincide with decreases in the CL. The CL varies significantly with increasing cloud optical depth only for optical depths of less than 5 for liquid water clouds. For ice clouds, the sensitivity is greatest for optical depths of less than 5, but changes in CL due to changes in cloud optical depth are still significant, even for larger optical depths. Ice clouds lead to greater warming at the surface than do liquid water clouds for optical depths of greater than about 6. Increases in cloud-top pressure or cloud fraction will lead to increases in the CL.

One or both of the CS or CL are not very sensitive to changes in surface temperature, effective particle radius, and liquid/ice water content, and so the CNET is also not very sensitive to those parameters (Figs. 8f–j). The CL is greater than the CS only for solar zenith angles greater than about 76° and 78° (Fig. 8d) and a visible surface reflectance of about 0.86 and 0.90 (Fig. 8a) for liquid water and ice clouds, respectively. We can, therefore, expect the net cloud radiative effect to change from cooling to warming when the surface is bright and the sun is low. The CNET is also negative over the entire range of cloud-top pressure (Fig. 8e), and its variation with changing cloud-top pressure is primarily governed by the relationship between the cloud-top pressure and the CL. The sensitivity of the surface cloud forcing to changes in cloud optical depth (Fig. 8c) and cloud fraction (Fig. 8b) is greater in the SW than in the LW so that the CNET decreases with increasing optical depth and cloud fraction.

In summary, the sensitivity of the CNET with respect to changing effective particle radius and cloud liquid/ice water content is fairly small. So, even though the effective particle radius and water content were kept fixed during the processing of the ISCCP D-series dataset and the water content was held constant during the APP-x processing, the errors in the CNET due to these assumptions should be small. In addition, the observed differences in cloud amount between the ISCCP-derived and APP-x datasets can certainly account for at least some of the differences in the CL and, hence, the CNET from the two datasets. Cloud optical depth and cloud-top pressure will also play a role. Because the CS has a strong solar zenith angle dependence and the ISCCP and APP-x observation times are different, the magnitude of the CS from the two sets will naturally be considerably different.

6. Summary

An ISCCP-derived dataset and the AVHRR-derived APP-x dataset were used to study the spatial and temporal variability of shortwave, longwave, and net cloud forcing at the surface in the Antarctic over a 9-yr period (1985–93). The accuracy of the ISCCP-derived and APP-x cloud forcing was assessed by validating shortwave, longwave, and net surface fluxes from the ISCCP-derived and APP-x data against surface measurements of upwelling and downwelling shortwave and longwave fluxes at two Antarctic stations. In addition, modeling studies were performed to determine the sensitivity of the shortwave, longwave, and net cloud forcing to

changes in various cloud and surface parameters associated with regional and/or global climate change.

It was found that the shortwave cooling effect of clouds on the surface is much greater over the ocean areas that surround the Antarctic continent than over the Antarctic continent itself. Over the Antarctic continent, the clear-sky net shortwave radiation at the surface is small when compared with the clear-sky net shortwave flux over the darker ocean surface because much of the downwelling shortwave radiation is reflected by the very bright snow surface. Thus, the difference between the net shortwave flux for cloudy conditions and clear sky will be smaller over the Antarctic continent when compared with the surrounding ocean for a given solar zenith angle. Because the amount of sunlight varies greatly throughout the year, the shortwave cloud forcing, especially over the ocean, will also.

Analysis of both datasets indicates that the longwave warming effect of clouds on the surface is not nearly as spatially or temporally variable as the shortwave cloud forcing is. This is especially true over the ocean areas, for which cloud cover does not vary much from month to month. The ISCCP-derived dataset indicates that the greatest longwave warming occurs in March over the ocean area south of 58.75°S and in April over the Antarctic continent. In the APP-x dataset, the greatest longwave warming was found in March over the ocean and in July over the Antarctic continent.

On the monthly timescale, clouds were found to have a warming effect on the surface of the Antarctic continent for every month of the year, which means that the longwave effect of clouds is larger than the shortwave effect of clouds for every month. This result is in contrast to the globally averaged effect, in which clouds cool the surface on an annual basis (Gupta et al. 1993; Rossow and Lacis 1990). The average of all of the ISCCP grid cells over the Antarctic continent for each month shows that clouds will warm the surface by as little as 0.04 W m^{-2} (December) or as much as 26 W m^{-2} (April and May). According to the APP-x results, the minimum warming is 16 W m^{-2} in March and the maximum warming is 30 W m^{-2} in July. Over the ocean poleward of 58.75°S, clouds were found to have a warming effect on the surface from March through October in the ISCCP-derived dataset and from April through September in the APP-x dataset. The model sensitivity study performed indicates that the differences in the net cloud forcing between the two datasets are likely due to differences in solar zenith angle, cloud amount, cloud-top pressure, and cloud optical depth. As an alternative, large differences in any of these parameters can account for the observed differences in the CNET between the two datasets.

The surface fluxes from both datasets were compared with measurements taken at the Neumayer and South Pole Stations. The net all-wave surface flux from the ISCCP-derived dataset was found to be within 3–50 W m^{-2} of the net all-wave flux calculated from measurements of upwelling and downwelling shortwave and longwave radiative fluxes at Neumayer Station on the monthly timescale. The largest errors occurred in the austral summer months. Further, the ISCCP-derived net all-wave surface flux was found to be within 0.4–50 W m^{-2} of the South Pole Station net all-wave flux. The APP-x net all-wave surface flux was found to be within 0.9–13 W m^{-2} of the Neumayer Station net all-wave flux and within 4–24 W m^{-2} of the South Pole Station net all-wave surface flux on the monthly timescale. Because the maximum overestimate in the net all-wave surface flux from the APP-x dataset is 12 W m^{-2} for either station and the average monthly minimum in the net cloud forcing over the Antarctic continent is 16 W m^{-2}, the conclusion that clouds have a warming effect on the surface over the Antarctic continent should be valid.

Model sensitivity studies, aimed at gaining insight about how the surface radiation budget in a cloudy atmosphere will change if certain cloud and surface properties were to change, were conducted. The results indicate that the net cloud forcing will be most sensitive to changes in cloud amount, surface reflectance, cloud optical depth, and cloud-top pressure for the case studied. The net cloud forcing will also be highly dependent on the solar zenith angle used in any calculations.

Acknowledgments. We thank Robert Stone for supplying the hourly measurements of surface fluxes at the South Pole and Jennifer Francis for useful discussions on cloud forcing. Dan Slayback and Veronica Fisher played important roles in the calculation of radiative fluxes from the ISCCP cloud product. Xuanji Wang assisted with the development of the extended APP product. The standard APP product was developed by James Maslanik, Chuck Fowler, and Jeff Key. APP data were provided by the National Snow and Ice Data Center. The measurements of surface fluxes at Neumayer Station were obtained from the Alfred Wegener Institute for Polar and Marine Research. This research was supported by NSF Grant OPP-0096085.

REFERENCES

Ambach, W., 1974: The influence of cloudiness on the net radiation balance of a snow surface with high albedo. *J. Glaciol.*, **13,** 73–84.

Curry, J. A., and E. E. Ebert, 1992: Annual cycle of radiation fluxes over the Arctic Ocean: Sensitivity to cloud optical properties. *J. Climate*, **5,** 1267–1280.

Dutton, E. G., R. S. Stone, and J. J. DeLuisi, 1989: South Pole surface radiation balance measurements, April 1986 to February 1988. NOAA Data Rep. ERL ARL-17, 49 pp.

Francis, J. A., and A. J. Schweiger, 2000: A new window opens on the Arctic. *Eos, Trans. Amer. Geophys. Union,* **81,** 77–83.

Gupta, S. K., W. F. Staylor, W. L. Darnell, A. C. Wilber, and N. A. Ritchey, 1993: Seasonal variation of surface and atmospheric cloud radiative forcing over the globe derived from satellite data. *J. Geophys. Res.,* **98,** 20 761–20 778.

Hines, K. M., R. W. Grumbine, D. H. Bromwich, and R. I. Cullather, 1999: Surface energy balance of the NCEP MRF and NCEP–

NCAR reanalysis in Antarctic latitudes during FROST. *Wea. Forecasting*, **14,** 851–866.

Key, J. R., 2002: The Cloud and Surface Parameter Retrieval (CASPR) system for polar AVHRR user's guide. Cooperative Institute for Meteorological Satellite Studies, University of Wisconsin—Madison, 61 pp.

——, and A. J. Schweiger, 1998: Tools for atmospheric radiative transfer: Streamer and FluxNet. *Comput. Geosci.*, **24,** 443–451.

——, and J. Intrieri, 2000: Cloud particle phase determination with the AVHRR. *J. Appl. Meteor.*, **39,** 1797–1805.

——, D. Slayback, C. Xu, and A. Schweiger, 1999: New climatologies of polar clouds and radiation based on the ISCCP ''D'' products. Preprints, *Fifth Conf. on Polar Meteorology and Oceanography*, Dallas, TX, Amer. Meteor. Soc., 227–232.

——, X. Wang, J. Stroeve, and C. Fowler, 2001: Estimating the cloudy sky albedo of sea ice and snow from space. *J. Geophys. Res.*, **106,** 12 489–12 497.

Li, Z., and H. G. Leighton, 1991: Scene identification and its effect on cloud radiative forcing in the Arctic. *J. Geophys. Res.*, **96,** 9175–9188.

Lubin, D., B. Chen, D. H. Bromwich, R. C. J. Somerville, W. Lee, and K. M. Hines, 1998: The impact of Antarctic cloud radiative properties on a GCM climate simulation. *J. Climate*, **11,** 447–462.

Maslanik, J. A., C. W. Fowler, J. R. Key, T. Scambos, T. Hutchinson, and W. Emery, 1998: AVHRR-based Polar Pathfinder products for modeling applications. *Ann. Glaciol.*, **25,** 388–392.

——, A. Lynch, and C. Fowler, 1999: Assessing 2-D and coupled-model simulations of sea ice anomalies using remotely-sensed Polar Pathfinder products. Preprints, *Fifth Conf. on Polar Meteorology and Oceanography*, Dallas, TX, Amer. Meteor. Soc., 476–479.

Meier, W. N., J. A. Maslanik, J. R. Key, and C. W. Fowler, 1997: Multiparameter AVHRR-derived products for Arctic climate studies. *Earth Interactions*, **1.** [Available online at http://EarthInteractions.org.]

Minnett, P. J., 1999: The influence of solar zenith angle and cloud type on cloud radiative forcing at the surface in the Arctic. *J. Climate*, **12,** 147–158.

Pavolonis, M. J., 2002: Antarctic cloud radiative forcing at the surface estimated from the ISCCP D1 and AVHRR Polar Pathfinder data sets, 1985–1993. M.S. thesis, Dept. of Atmospheric and Oceanic Sciences, University of Wisconsin—Madison, 123 pp. [Available from University of Wisconsin—Madison, 1225 West Dayton St., Madison, WI 53706.]

Rossow, W. B., and A. A. Lacis, 1990: Global, seasonal cloud variations from satellite radiance measurements. Part II: Cloud properties and radiative effects. *J. Climate*, **3,** 1204–1253.

——, A. W. Walker, D. E. Beuschel, and M. D. Roiter, 1996: International Satellite Cloud Climatology Project (ISCCP) documentation of cloud data. Tech. Doc., World Climate Research Programme, WMO, 115 pp.

Schiffer, R. A., and W. B. Rossow, 1983: The International Satellite Cloud Climatology Project (ISCCP): The first project of the World Climate Research Programme. *Bull. Amer. Meteor. Soc.*, **64,** 779–784.

Schweiger, A. J., and J. R. Key, 1994: Arctic Ocean radiative fluxes and cloud forcing estimated from the ISCCP C2 cloud dataset, 1983–1990. *J. Appl. Meteor.*, **33,** 948–963.

Toon, O. B., C. P. McKay, and T. P. Ackerman, 1989: Rapid calculation of radiative heating rates and photodissociation rates in inhomogeneous multiple scattering atmospheres. *J. Geophys. Res.*, **94,** 16 287–16 301.

Tsay, S. C, 1986: Numerical study of the atmospheric radiative transfer process with application to the Arctic energy balance. University of Alaska, Geophysical Institute Rep. UAG R-307, 193 pp.

——, K. Stamnes, and K. Jayaweera, 1989: Radiative energy budget in the cloudy and hazy Arctic. *J. Atmos. Sci.*, **46,** 1002–1018.

Zhang, T., K. Stamnes, and S. A. Bowling, 1996: Impact of clouds on surface radiative fluxes and snowmelt in the Arctic and subarctic. *J. Climate*, **9,** 2110–2123.